A chemotactic pollution-homing UAV guidance system

Oscar Alvear Alvear, Nicola Roberto Zema, Enrico Natalizio, Carlos T Calafate

A chemotactic pollution-homing UAV guidance system

Oscar Alvear Alvear*, Nicola Roberto Zema†, Enrico Natalizio †, Carlos T. Calafate *
* Department of Computer Engineering, Universitat Politècnica de València, Camino de Vera, S/N, 46022 Valencia, Spain
e-mail: osal@doctor.upv.es; calafate@disca.upv.es
† Sorbonne Universités, Université de technologie de Compiègne, CNRS, UMR 7253 Heudiasyc
60200 Compiègne, France. e-mail: {nicola.zema,enrico.natalizio}@hds.utc.fr

***Abstract*—Due to their deployment flexibility, Unmanned Aerial Vehicles have been found suitable for many application areas, one of them being *air pollution monitoring*. In fact, deploying a fleet of Unmanned Aerial Vehicles (UAVs) and using them to take environmental samples is an approach that has the potential to become one of the key enabling technologies to enforce pollution control in industrial or rural areas. In this paper, we propose to use an algorithm called Pollution-driven UAV Control (PdUC) that is based on a chemotaxis metaheuristic and a Particle Swarm Optimization (PSO) scheme that only uses local information. Our approach will be used by a monitoring Unmanned Aerial Vehicle to swiftly cover an area and map the distribution of its aerial pollution. We show that, when using PdUC, an implicit priority is applied in the construction of pollution maps, by focusing on areas where the pollutants' concentration is higher. In this way, accurate maps can be constructed in a faster manner when compared to other strategies. We compare PdUC against various standard mobility models through simulation, showing that our protocol achieves better performances, by finding the most polluted areas with more accuracy, within the time bounds defined by the UAV flight time.**

***Keywords*—UAV Guidance, Chemotaxis, Air Pollution.**

I. Introduction

Air pollution monitoring has become an issue of utmost importance in the last decades since the world has witnessed an increase of pollutants, as well as their impact on health-related problems [1].

The use of dedicated architectures and hardware for pollution monitoring in inhabited areas is outmatched, in theory, only by the use of crowdsensing [2]. However, the majority of methods, used insofar, to keep track of air pollution in major cities, rely on fixed monitoring stations [3] and these traditional methods are slowly being replaced by ground-vehicle-based mobile sensors. These latter ones would theoretically be able to cover the same areas as the former, while employing a reduced number of sensors, as opposed to the solution with fixed stations.

In respect to the widespread use of small pollution monitoring sensors embedded on mobile vehicles, the possible scenarios of their use can be divided in two main classes: (i) urban environments, where it is possible to embed the sensors on a wide set of vehicles like bicycles [4] or cars [5]; and (ii) rural and industrial areas, where vehicular traffic is scarce and limited to the main transportation arteries. In the latter case, furthermore, crowdsensing often fails to provide enough data to obtain realistic measurements having the required granularity. In the case of large urban or industrial areas, a fleet of mobile vehicles could be efficiently used to cover the vast distances associated with them. The use of autonomous sensor carriers is even more encouraged, in the last case, thanks to the following considerations: (i) the relative absence of civilian population to be taken care of during robotic operations; (ii) stable and regulated positioning of obstacles; (iii) less constraints in terms of UAV flight laws and, finally, (iv) safety and security issues, since some areas could be dangerous for human operation. In these environments, ground access is usually hindered and the most feasible way to implement a fleet of mobile pollution-monitoring robots is via Unmanned Aerial Vehicles (UAVs). It is important, at this point, to distinguish that through all the paper we always refer to *small* UAVs. In this category belong all the robots commercially available for small civil application such as quad- and octa-rotors. We restrain to apply our studies to the much more sophisticated autonomous flying machines of heavy industrial and military applications.

In this paper we propose the use of UAVs as the way to implement an air pollution monitoring service that leverages the use of bio-inspired approaches as the main robotic control strategy. We show that, using a chemotaxis-based approach for the drone movement control, it is possible to achieve faster and more accurate estimates of the position of the most polluted areas, with respect to classical area-search approaches. Our analysis also takes into account uncertainty-based considerations in the sensor sampling operations. This paper is organized as follows: in section II we refer to some related works addressing UAV-based sensing, UAV mobility models, and UAV control protocols. Section III presents the description of our proposal. In section IV, we compare our algorithm against the Billiard and Spiral mobility models via simulations. Section V discusses the open issues in air pollution monitoring using UAVs. Finally, in section VI, we present the conclusions of our work.

II. Related Works

The last decade saw a blossoming of UAV applications. The NASA [6] conducted a set of studies about the *Civil Application* possibilities for flying drones, determining that the

following application categories would benefit the most from *small-UAV* development: commercial, earth science, national security and land management. In addition, there are several works analyzing the uses of small UAVs; for instance, the studies of Hugenholtz et al. [7] show the various possibilities of using UAVs for Earth Sciences and Remote Sensing.

Focusing on our topic, despite the presence of several works related to *air pollution monitoring using Unmanned Aerial Systems (UAS)*, the topics addressed in the majority of them involve, mainly, swarm creation or communication/interaction issues. For example, in [8], its Authors propose a mobility model for a group of nodes following Virtual Tracks (highways, valley, etc.) operating in a predefined Switch Station mode, through which nodes can split or merge with another group of nodes.

If we analyze works related to mobility models for UAS that could be used for air pollution monitoring tasks, we can observe that, at the best of the authors' knowledge, no work is optimized or based on coverage improvement for a certain area.

For instance, in [9], its Authors propose a mobility model based on the *Enhanced Gauss-Markov* model to eliminate and limit sudden stops and sharp turns that the random waypoint mobility model typically creates. Also, in [10], authors present a *semi-random circular movement* (SRCM) based model, analyzing the coverage and network connectivity by comparing it against the random waypoint mobility model. The authors of [11] compare random waypoint-based, Markov-based and Brownian motion-based algorithms to cover a specific area, analyzing the influence of physical collision avoidance systems in the area covering completion time. The work in [12] compares the results of using Random Mobility Model and the Distributed Pheromone Repel Mobility Model as direction decision engines (next way-point) in UAV environments. The authors of [13] propose an algorithm to cover a specific area: it selects a point in space along with the line perpendicular to its heading direction, and then drives the UAV on the basis of geometric considerations. There are works for specifics tasks such as [14], where authors present a mobility model for the self-deployment of an *Aerial Ad Hoc Network* in a disaster recovery scenario in order to create a flying and flexible communications infrastructure that victims can use. The mobility model proposed there is mainly built on the Jaccard dissimilarity metric, to control the deployment of the Unmanned Aerial Vehicles composing the network. A similar work is presented in [15], where instead an *in-network density analysis* is used to select the physical areas than need to be visited by a flying robot. There are also studies following animal-based navigation patterns. An example of such a work is [16], where authors investigate the UAV placement and navigation strategies with the end goal of improving network connectivity, using local flocking rules that *aerial living beings* like birds and insects seem to follow. The use of UAVs for air pollution monitoring in a specific area is, however, still not present in scientific literature, and this work can be seen as one of the first approaches in this direction.

III. Overview of the proposed solution

Chemotaxis metaheuristics are based on bacteria movement, which react to a chemical stimulus by moving towards areas with a higher concentration of given components (e.g. food), or moving away from some others (e.g. poison) [17]. Let us consider an agent i moving on a Euclidean plane, located at position $\overrightarrow{P}_{i,j}$ from an absolute reference axis, and moving along time in sequential steps j. For every chemotactic step, a new position $\overrightarrow{P}_{i,j}$ is calculated based on the the previous one $\overrightarrow{P}_{i,j-1}$, plus a step size d_j applying a random direction θ_j, as specified in equation 1.

$$\overrightarrow{P}_{i,j} = \overrightarrow{P}_{i,j-1} + d_i \times \theta_{i,j} \tag{1}$$

$$\theta_{i,j} = \begin{cases} \theta_{i,j-1} + \alpha_{i,j} & p_{i,j} \geq p_{i,j-1} \\ -\theta_i(j-1) + \beta_{i,j} & p_{i,j} < p_{i,j-1} \end{cases} \tag{2}$$

The direction $\theta_{i,j}$, as shown in equation 2, is calculated based on the concentration of a certain chemical component, sampled by an agent i at the time step j: $p_{i,j}$. With respect to the previous sampled value $p_{i,j-1}$, the following two types of movements are contemplated: Run and Tumble. In the former, Run, when the component concentration is increasing with respect to the previous value, the movement continues to follow the same direction as before ($\theta_{i,j-1}$) plus a random angle $\alpha_{i,j}$. For the latter, Tumble, when the concentration is decreasing, the movement takes a turn in the inverse direction $-\theta_{i,j-1}$, plus a random angle $\beta_{i,j}$. Notice that both $\alpha_{i,j}$ and $\beta_{i,j}$ are used to introduce variability and to maximize the gradient.

The use of rotating-wing UAVs, equipped with chemical sensors and tasked to survey large areas, could follow chemotactic mobility patterns since their flight behavior could easily implement the following two-phase algorithm: first, it reads a pollution concentration while hovering; next, it follows a chemotactic step.

In this context, we have developed an algorithm called Pollution-driven UAV Control (PdUC) based mainly on the chemotaxis metaheuristic concept to search an area for the highest pollution concentration level. Once this area is found, the flying drone covers the area following a spiral movement, starting from the most polluted area. Our algorithm is composed of two phases: (i) A *Search* phase, in which the UAV searches for a globally maximum pollution value, and (ii) An *Explore* phase, where the UAV explores the surrounding area, following a spiral movement, until it covers the whole area, until the allowed flight time ends or until it finds another maximum value, in which case it returns to the *Search* phase.

The *Search* phase is based on two concepts: a chemotaxis metaheuristic, and a local Particle Swarm Optimization algorithm. Initially, before the UAV starts its first movement, it samples the pollution value and puts it in a buffer. For each chemotactic step, it starts to hover, collects another sample, and compares it with the previous one. If the sampling variation is positive (increasing), the UAV follows a "Run"

chemotaxis direction, with a random $\alpha_{i,j}$ of $[-30, 30]$ degrees. Otherwise, if the sampling variation is decreasing, the UAV calculates the "Tumble" chemotaxis direction in the reverse orientation with a random $\beta_{i,j}$ of $[-150, 150]$, although modified by the actual maximum value reached (md_i), as shown in Figure **??**. Equation 3 denotes the formula to calculate the new direction, and γ specifies the weight of the md_i, which must be between 0 and 1.

To determine when PdUC has found a maximum local value, we use a ttl. When PdUC finds a maximum value, we reset the ttl, which then increases until it finds new maximum pollution values, or until reaching the maximum ttl value, in which case PdUC changes to the exploration phase since it considers that a local maximum value has been found.

$$\theta_{i,j} = \begin{cases} \theta_{i,j-1} + \alpha_{i,j} & \text{Run} \\ (1-\gamma)(-\theta_{i,j-1} + \beta_{i,j}) + \gamma md_i & \text{Tumble} \end{cases} \quad (3)$$

Once a maximum value is reached, the next phase is to *Explore* the surrounding area by following an archimedean spiral: starting from the maximum value, covers the surrounding area by applying a basic step size d_j, and changing it depending on the detected pollution variations, a procedure that is similar to the finding phase. If the variation is less than a preset value c_i, the step size increases until reaching $3 \times d_j$; otherwise, it decreases until d_j is reached. If a maximum pollution value is found, PdUC automatically returns to the exploration phase. Finally, once the whole area is covered, the UAV changes to a *return to home* mode to finish the exploration.

Figure 1 summarizes the operation of the algorithm and displays the separation between the *Search* and the *Explore* phases.

IV. Validation & Simulation

To validate our protocol, we have run several simulations with different configurations.

To prepare a suitable data environment, we have created various distribution maps of pollution sources using *R Graph* [18]. The maps are created following a kriging-based interpolation of a Gaussian distribution from random data sources, with values between 40 and 180 ppb, thereby simulating a typical ozone distribution.

Figure 3 shows some samples of the created maps.

Using the previously created data as input, we have run several simulations using OMNeT++, comparing our protocol against both the Billiard and Spiral mobility patterns. In the simulator, we have created a mobility model implementing PdUC. To simulate the sampling process, we have tuned OMNeT++ to periodically take the values from the pollutant distribution map.

We analyze the results of the three different movement patterns (PdUC, Spiral, and Billiard) creating distribution pollution maps using their samplings, and comparing against the original map. The maps are created via the R Graph tool using kriging-based interpolation.

Table IV summarizes the parameters used in the simulations.

Parameter	Value
Area	4x4 Km
Pollution distribution	Kriging-based
Pollution range	[40 - 180] ppb
Pollution oscillation	10 ppb
Mobility base	Waypoint
Speed	Constant (20 m/s)
Monitoring time	4 seconds
Step distance	100 m
Mobility models	Billiard, Spiral and PdUC

Since we are proposing the PdUC algorithm for industrial environments, the simulation area defined is a 4×4 Km area with no obstacles as the drones flight well above ground. We introduce random variations into the sampling process to simulate the inaccuracies of off-the-shelf sensors. In our simulation we set the maximum UAV speed to 20 m/s, a value achievable by many commercial UAVs. The step distance defined between consecutive samples is 100 meters. Once a new sampling location is reached, the monitoring time per sample is defined to be 4 seconds.

The mobility models used are Billiard, Spiral and PdUC. These models have different assumptions regarding the initial UAV position. In the Billiard model, the UAV starts in a corner of the target area and then covers the whole area. The spiral model is similar, but it starts at the center of the area to cover. Finally, PdUC is set to start at a random position within the target area.

We now proceed by analysing the time required to cover the entire area using each of the approaches being tested. For this purpose, we averaged 100 simulations for each model (Billiard, Spiral and PdUC, with each drone starting at random position), trying to determine the required time to completely cover the area.

Figure **??** shows the Cumulative Distribution Function relative to the time to cover the whole area for the three mobility models. It can be seen that the Billiard and Spiral models do not depend on the starting position, spending a nearly constant time (5600 and 2600 seconds, respectively) for each established configuration. In the case of the PdUC mobility model, since it reacts to air pollution, the time required to cover the complete area varies between 1800 and 4300 seconds, depending on the starting position.

Due to battery restrictions, it is interesting to analyze how fast each mobility model discovers the most polluted areas, and how accurately does it recreate the pollution distribution. For this purpose, we analyze the relative error for the three mobility models at different time instants (600, 1200, 1800, 2400, 3000 and 6000 seconds); this error is defined as shown in equation 4:

$$e_t = \frac{\sum_{i=1}^{m} \sum_{j=1}^{n} \left| \frac{s_{x,y,t} - b_{x,y}}{\triangle b} \right|}{m \cdot n} \quad (4)$$

where, e_t is the relative error at time t; $s_{x,y,t}$ is the recreated pollution value using the simulation until time t at position

(x, y), $b_{x,y}$ is the reference pollution value at position (x, y), and n and m are the dimensions of the target area, respectively.

Figure **??** shows the time evolution of the relative error between the three mobility models (Billiard, Spiral, and PdUC) and the original one. We can observe that all mobility models have roughly the same behavior: they start with a high relative error, which is expectable since we are using kriging interpolation to recreate the pollution distribution, and it tends to the mean value when the number of samples is not enough. Then, as more samples become available, the spatial interpolation process quickly becomes more precise.

Although the three mobility models are similar, the spiral approach achieves a better performance in terms of relative error reduction. However, if we analyze only the most polluted areas, that is, the values higher than a certain threshold (120 and 150, in our case, based on AQI [19]), we find that PdUC provides better results.

Figures 6 and 7 show the comparison between the Billiard, Spiral, and PdUC mobility models at different times when only focusing on air pollution values higher than 120 and 150 ppb, respectively. These results show that PdUC provides better results than the Billiard and Spiral movement patterns, outperforming their accuracy from nearly the beginning of the experiment (1200 seconds), and reaching the lowest relative error values in just 3600 seconds, with these two other mobility approaches more than doubling the error values for a same time. In particular, the Billiard mobility pattern requires about 6000 seconds to achieve a similar degree of accuracy (120 ppb case), while the Spiral approach is not able to achieve values as low as PdUC in any of the cases. This occurs because PdUC focuses on the highest values in the chemotaxis-based phase. PdUC always prioritizes the most polluted areas in detriment of less polluted ones allowing to obtain, at least, some area with the highest pollution values.

V. Open Issues

Unmanned Aerial Systems (UAS) have quickly expanded in different areas due to their flexibility and relatively low costs. Previously, we had proposed the use of UAVs for air pollution monitoring [20] by equipping them with off-the-shelf sensors. Now, in the current paper, we are introducing an algorithm called PdUC to guide a single UAV to monitor a specific area. However, there are still several open issues related to this topic.

Until now, we have considered the operations of a single UAV. The next step in our research is to introduce multiple-UAVs and their cooperation schemes. By following this research line, the following aspects need to be immediately addressed:

- **Cooperation:** to maximize the effectiveness and reduce mapping times, it is advisable to have several UAVs that cooperate with each other to achieve a same task, thereby accelerating the whole process and avoiding battery exhaustion.
- **Collision Avoidance:** a correct coordination between nearby UAVs is required to avoid collisions when flying in a close range.
- **Communications:** to achieve the aforementioned goals of cooperation and collision avoidance, communications between UAVs, and between UAVs and a central management unit, are required.

On the other hand, using mobile sensors installed on UAVs introduces new aspects to consider in the sensing process:

- **Altitude:** despite currently most pollution studies are made at ground level, the use of UAVs allows determining the concentration of pollutants at different heights, which helps at finding out whether there are layers of pollutants that can cause health problems.
- **Influence of the wind:** the sampling procedure includes sensors that are sensitive to wind conditions. In addition, wind causes the overall pollution map to be more dynamic. In this context, both issues deserve more scrutiny.

VI. Conclusions

Recently, Unmanned Aerial Systems have experienced unprecedented growth, offering a platform for the fast development of solutions due to their flexibility and relatively low cost; they can be a good option to solve the previous requirements allowing to monitor remote areas with difficult access.

In previous works [20], we proposed to equip UAVs with off-the-shelf sensors for monitoring tasks, but the guidance system was still missing. To solve this issue, we have proposed adopting the Pollution-based UAV Control system (PdUC), which allows us to monitor a specific area focusing on the most polluted zones.

PdUC is based on a Chemotaxis metaheuristic and a local Particle Swarm Optimization (PSO) concepts, creating an algorithm able to quickly find areas with high pollution values, and to cover the surrounding area as well, thereby obtaining a complete and detailed pollution map.

To validate our proposal, we compared our approach against the Billiard and Spiral mobility models through simulations implemented in OMNeT++. The simulation experiments show that PdUC offers significantly better performance at reducing prediction errors, especially concerning the high-value range.

We further identified what needs to be immediately addressed to lead on and complete our research and we plan to pursue it in publications to come.

Acknowledgment

This work has been partially carried out in the framework of the DIVINA Challenge Team, which is funded under the Labex MS2T program. Labex MS2T is supported by the French Government, through the program Investments for the future managed by the National Agency for Research (Reference: ANR-11-IDEX-0004-02). This work was also supported by the "Programa Estatal de Investigación, Desarrollo e Innovación Orientada a Retos de la Sociedad, Proyecto I+D+I TEC2014-52690-R", and by the "Programa de becas SENESCYT de la República del Ecuador".

REFERENCES

[1] A. Seaton, D. Godden, W. MacNee, and K. Donaldson, "Particulate air pollution and acute health effects," *The lancet*, vol. 345, no. 8943, pp. 176–178, 1995.

[2] O. Alvear, W. Zamora, C. Calafate, J.-C. Cano, and P. Manzoni, "An architecture offering mobile pollution sensing with high spatial resolution," *Journal of Sensors*, vol. 2016, 2016.

[3] P. S. Kanaroglou, M. Jerrett, J. Morrison, B. Beckerman, M. A. Arain, N. L. Gilbert, and J. R. Brook, "Establishing an air pollution monitoring network for intra-urban population exposure assessment: A location-allocation approach," *Atmospheric Environment*, vol. 39, no. 13, pp. 2399–2409, 2005.

[4] S. B. Eisenman, E. Miluzzo, N. D. Lane, R. A. Peterson, G.-S. Ahn, and A. T. Campbell, "Bikenet: A mobile sensing system for cyclist experience mapping," *ACM Transactions on Sensor Networks (TOSN)*, vol. 6, no. 1, p. 6, 2009.

[5] M. Pujadas, J. Plaza, J. Teres, B. Artuñano, and M. Millan, "Passive remote sensing of nitrogen dioxide as a tool for tracking air pollution in urban areas: the madrid urban plume, a case of study," *Atmospheric Environment*, vol. 34, no. 19, pp. 3041–3056, 2000.

[6] T. H. Cox, C. J. Nagy, M. A. Skoog, I. A. Somers, and R. Warner, "Civil uav capability assessment."

[7] C. H. Hugenholtz, B. J. Moorman, K. Riddell, and K. Whitehead, "Small unmanned aircraft systems for remote sensing and earth science research," *Eos, Transactions American Geophysical Union*, vol. 93, no. 25, pp. 236–236, 2012.

[8] B. Zhou, K. Xu, and M. Gerla, "Group and swarm mobility models for ad hoc network scenarios using virtual tracks," in *Military Communications Conference. MILCOM 2004.*, vol. 1, pp. 289–294, IEEE, 2004.

[9] J.-D. M. M. Biomo, T. Kunz, and M. St-Hilaire, "An enhanced gauss-markov mobility model for simulations of unmanned aerial ad hoc networks," in *Wireless and Mobile Networking Conference (WMNC), 2014 7th IFIP*, pp. 1–8, IEEE, 2014.

[10] W. Wang, X. Guan, B. Wang, and Y. Wang, "A novel mobility model based on semi-random circular movement in mobile ad hoc networks," *Information Sciences*, vol. 180, no. 3, pp. 399–413, 2010.

[11] D. Orfanus and E. P. de Freitas, "Comparison of uav-based reconnaissance systems performance using realistic mobility models," in *2014 6th International Congress on Ultra Modern Telecommunications and Control Systems and Workshops (ICUMT)*, pp. 248–253, IEEE, 2014.

[12] E. Kuiper and S. Nadjm-Tehrani, "Mobility models for uav group reconnaissance applications," in *2006 International Conference on Wireless and Mobile Communications (ICWMC'06)*, pp. 33–33, IEEE, 2006.

[13] Y. Wan, K. Namuduri, Y. Zhou, and S. Fu, "A smooth-turn mobility model for airborne networks," *IEEE Transactions on Vehicular Technology*, vol. 62, no. 7, pp. 3359–3370, 2013.

[14] S. Toral, D. Reina, F. Barrero, *et al.*, "A self organising aerial ad hoc network mobility model for disaster scenarios," in *Developments of E-Systems Engineering (DeSE), 2015 International Conference on*, pp. 35–40, IEEE, 2015.

[15] O. Briante, V. Loscri, P. Pace, G. Ruggeri, and N. R. Zema, "COMVIVOR: An Evolutionary Communication Framework Based on Survivors' Devices Reuse," *Wireless Personal Communications*, vol. 85, no. 4, pp. 2021–2040, 2015.

[16] P. Basu, J. Redi, and V. Shurbanov, "Coordinated flocking of uavs for improved connectivity of mobile ground nodes," in *Military Communications Conference, 2004. MILCOM 2004. 2004 IEEE*, vol. 3, pp. 1628–1634, IEEE, 2004.

[17] J. Taktikos, H. Stark, and V. Zaburdaev, "How the motility pattern of bacteria affects their dispersal and chemotaxis," *PLOS ONE*, vol. 8, pp. 1–8, 12 2014.

[18] R Core Team, *R: A Language and Environment for Statistical Computing*. R Foundation for Statistical Computing, Vienna, Austria, 2016.

[19] U. S. E. P. Agency, "Air Quality Index Available: http://cfpub.epa.gov/airnow/index.cfm?action=aqibasics.aqi," 2015.

[20] O. Alvear, C. T. Calafate, E. Hernández, J.-C. Cano, and P. Manzoni, "Mobile pollution data sensing using uavs," in *Proceedings of the 13th International Conference on Advances in Mobile Computing and Multimedia*, pp. 393–397, ACM, 2015.

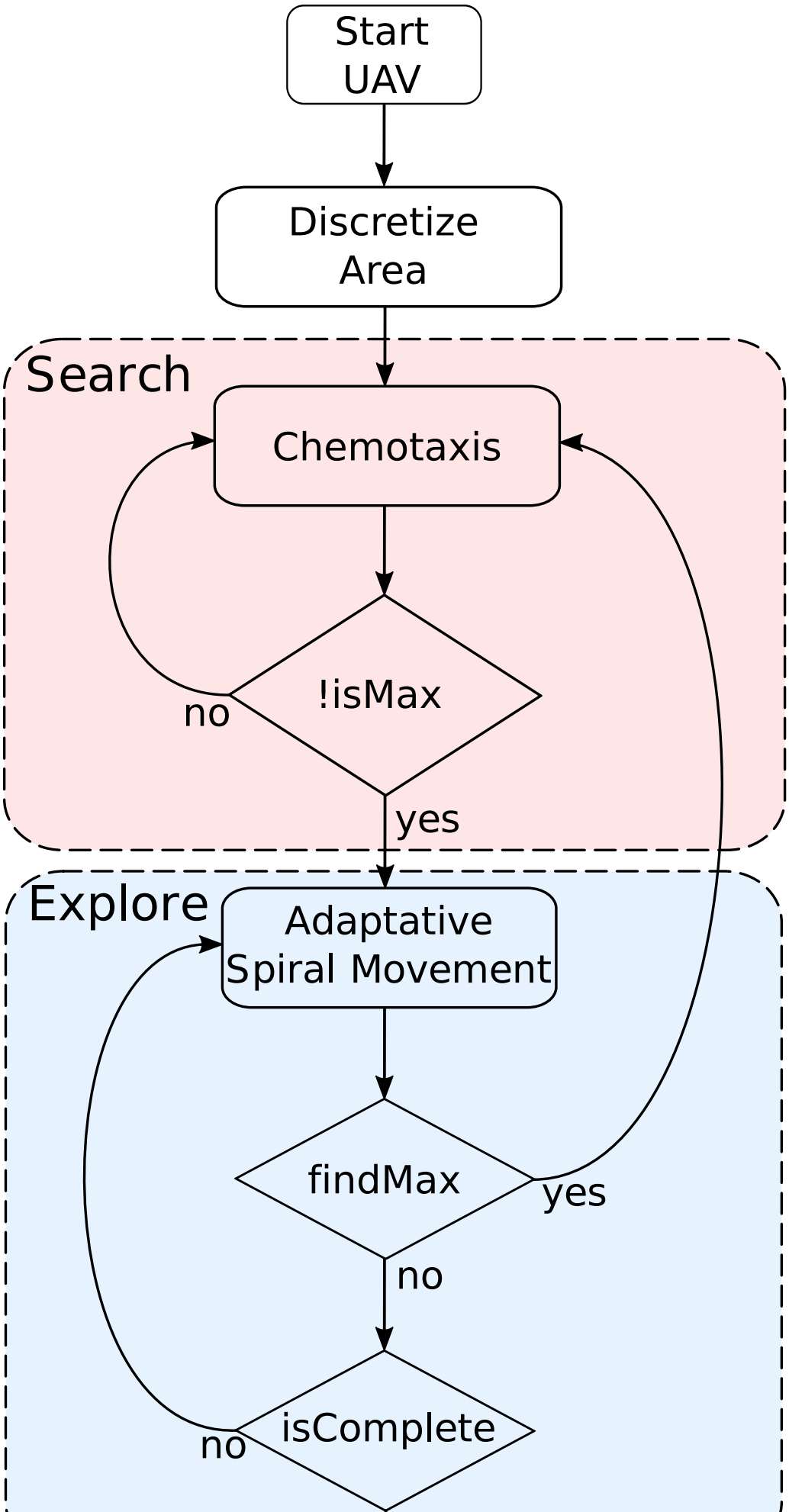
Start
UAV
Discretize
Area
Search
Chemotaxis
!isMax
no
yes
Explore
Adaptative
Spiral Movement
findMax
yes
no
isComplete
no

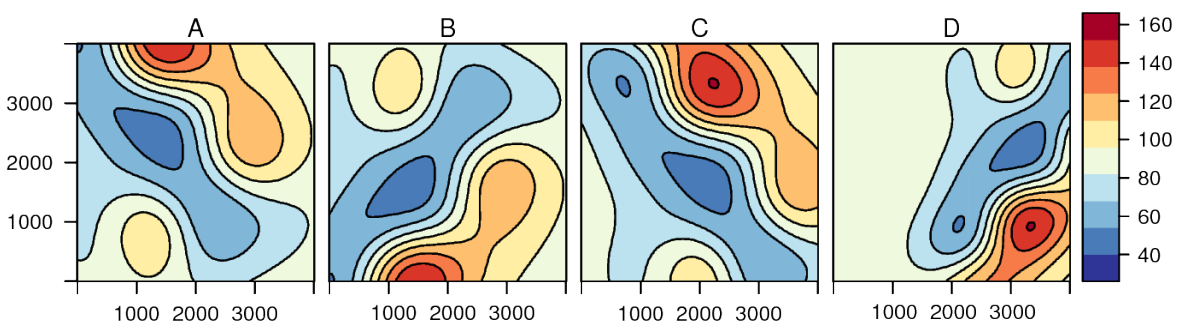

Fig. 3. Pollution distribution examples used to validate PdUC against Billiard and Spiral mobility models.

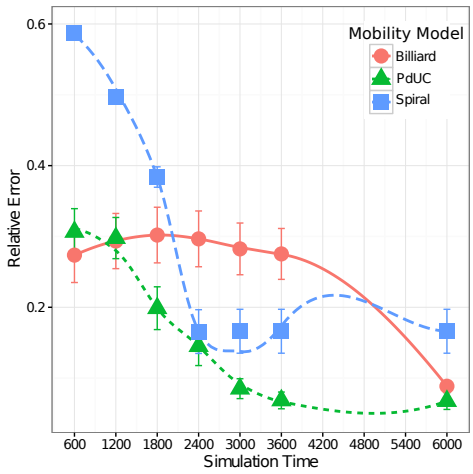

Fig. 6. Relative error comparison between PdUC, Billiard, and Spiral mobility models at different times when only analyzing values higher than 120 ppb.

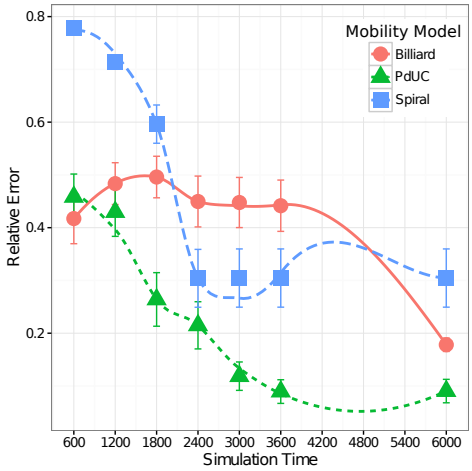

Fig. 7. Relative error comparison between PdUC, Billiard, and Spiral mobility models at different times when only analyzing values higher than 150 ppb.